Probing the Reactivity of the Active Material of a Li-ion Silicon Anode with Common Battery Solvents

Journal:	*ACS Applied Materials & Interfaces*
Manuscript ID	am-2021-01151j.R2
Manuscript Type:	Article
Date Submitted by the Author:	n/a
Complete List of Authors:	Han, Binghong; Argonne National Laboratory, Chemical Science and Engineering Zhang, Yunya; Argonne National Laboratory, Chemical Sciences and Engineering Liao, Chen; Argonne National Lab, Trask, Stephen; Argonne National Laboratory, Chemical Sciences and Engineering and Cell, Analysis, Modeling, and Prototyping (CAMP) Facility li, xiang; Argonne National Laboratory, Chemical Science and Engineering Uppuluri, Ritesh; Argonne National Laboratory, Chemical Sciences and Engineering Vaughey, John; Argonne National Lab, Chemical Sciences and Engineering Key, Baris; Argonne National Laboratory, Chemical Sciences and Engineering Division Dogan, Fulya; Argonne National Laboratory, Chemical Science and Engineering Division

Probing the Reactivity of the Active Material of a Li-ion Silicon Anode with Common Battery Solvents

Binghong Han*, Yunya Zhang, Chen Liao, Stephen E.Trask, Xiang Li, Ritesh Uppuluri, John T. Vaughey, Baris Key* , Fulya Dogan *

Chemical Sciences and Engineering Division, Argonne National Laboratory, Lemont, IL 60439, United States

*hbhtiancai@gmail.com, bkey@anl.gov, fdogan@anl.gov

ABSTRACT

Calculations and modeling have shown that replacing the traditional graphite anode with silicon can greatly improve the energy density of lithium-ion batteries. However, large volume change of silicon particles and high reactivity of the lithiated silicon when in contact with the electrolyte leads to rapid capacity fading during charging/discharging processes. In this report, we use specific lithium silicides (LS) as model compounds to systematically study the reaction between lithiated Si and different electrolyte solvents, which provides a powerful platform to deconvolute and evaluate the degradation of various organic solvents in contact with the active lithiated Si electrode surface after lithiation. Nuclear magnetic resonance characterization results show that a cyclic carbonate such as ethylene carbonate is chemically less stable than a linear carbonate such as ethylmethyl carbonate, and fluoroethylene carbonate, and triglyme as they are found to be more stable when mixed with LS model compounds. Guided by the experimental results, two EC-free electrolytes are studied, and the electrochemical results show improvements with graphite-free Si electrodes relative to the traditional ethylene-carbonate based electrolytes. More importantly, the study contributes to our understanding of the significant fundamental chemical and electrochemical stability differences between silicon and traditional graphite lithium-ion battery (LIB) anodes and suggests a focused development of electrolytes with specific chemical stability versus lithiated silicon which can passivate the surface more effectively.

KEYWORDS

Lithium Silicide, Silicon Anode Solvents, NMR, EC, Triglyme, FEC, EMC.

I. INTRODUCTION

The development of next-generation lithium-ion batteries with higher density and energy efficiency has become one of the main challenges in modern electrochemical materials research with the increased demands of the rapidly emerging electric vehicle markets and next-generation portable electronic devices. One effective way to gain higher cell capacity and energy density is to replace the traditional graphite anode with higher capacity materials such as the Si anodes, with theoretical capacity (~3600 mAh/g) 10 times higher than that of graphite (~370 mAh/g)[1-4]. In addition to its electrochemical properties, silicon is inexpensive and earth abundant, making it a viable replacement for carbon anodes[1]. Despite numerous advantages of Si anode materials, in practice, Si anodes suffer from several physical disadvantages including large volume change (up to 400%) during the charging-discharging cycling, and formation of various highly reactive lithium silicides (LS) as charged intermediates that contain highly reactive Si_2^{-2} and/or Si^{-4} anions that have been reported to react with and reduce the commonly used binders and electrolyte components.[5-9] This consequential disintegration of the anode electrode structure and the instabilities it brings to the solid-electrolyte interphase (SEI) leads to the continuous active Li loss as well as continuous decomposition/depletion of electrolytes, a main cause of rapid capacity fade in Si electrodes[1, 4, 10-12]. One potential solution is to engineer the active silicon materials by synthesizing nano-scale materials or porous structures, or by embedding the silicon in a Si-carbon composite, hollow carbon sphere, or within Si-metal alloys. These strategies also help release particle strain and avoid fractures during the lithiation/delithiation process.[4, 13-15] Additionally, the stabilization of the silicon anode via the formation of stable Li–M–Si ternaries is an alternative to mitigate the high reactivity of lithium silicides causing electrode degradation and long term cyclability issues. In our previous study, we used inorganic compounds as a secondary salt (such as 0.1 M $M(TFSI)_x$ (M = Mg, Zn, Al and Ca)) in a traditional electrolyte leading in situ formation of Li–M–Si ternaries, which effectively lowers the reactivity of lithiated silicon with electrolyte, binder and other cell components, reducing side reactions and Li loss which then, enables stable cyclability and calendar life with a higher coulombic efficiency [16].

Another approach is to use binders that contain carboxy groups, such as carboxymethylcellulose (CMC), polyacrylic acid (PAA), and lithiated PAA (LiPAA), which are less reactive in contact with the charged Si anodes and are thought to exhibit a self-healing effect upon local structure damage particles [17-20]. At the same time, many researchers are working on the development of Si-anode-compatible electrolytes that can form a stable and elastic SEI to withstand the large volume fluctuations during the cycling. The most studied electrolyte additives for Si-based electrode are fluoroethylene carbonate (FEC), vinylene carbonate (VC), lithium bisoxalatoborate (LiBOB), succinic anhydride (SA), and methylene-ethylene carbonate (MEC) which have been noted to change the chemistry and structure of the SEI to

stabilize the SEI layer and improve the capacity retention of Si anodes.[21-28] Alternatively, replacing the most reactive solvents in the solvent mixture, such as ethylene carbonate (EC), with some less-reactive solvents, such as methylene-ethylene carbonate (MEC) and FEC in the electrolyte, has been evaluated as an alternative to extending the performance of this anode system. [22, 27, 28] Despite the large amount of studies focused on the designing of new electrolytes and understanding decomposition products of EC and FEC solvents for silicon anodes [29, 30, 31] there is limited understanding available that describes the reactivity and degradation mechanism of different electrolyte solvents in contact with the amorphous or crystalline LS formed during the lithiation of Si anodes, which is one of the main causes of inefficiencies related to Si anodes. [5-9,16] This lack of a complete understanding is due to the complexity of different battery components (including binders, salts, solvents, etc.) in contact with the lithiated Si electrodes and causing the formation of various compounds in the SEI layer.

In this study, we investigated the potential chemical reactions between LS model compounds and different relevant and commonly used electrolyte solvents, including EC, ethylmethyl carbonate (EMC), triglyme (TG), and FEC, with two different salts, $LiPF_6$ and LiTFSI, to stabilize the lithiated Si anodes in Li-ion batteries. To deconvolute the LS-electrolyte interactions from the reaction between charged Si anode and other battery components, we synthesized crystalline LS with the intermediate stoichiometry of Li_7Si_3 as a model compound (the dominant phase near 300mV vs. Li) to directly interact with the organic solvent via physical mixing in an inert atmosphere. We believe this approach is crucial to understand the interaction and reactivity of lithium silicides and electrolyte/electrode components and a key step for their optimization studies.

Among all the tested solvents, EC was found to be the most reactive in contact with LS, while TG, EMC, and FEC were found to be noticeably less reactive. This suggests EC as a contributor, causing the most severe degradation issues when charging the Si anode to low (even moderate anode) voltages. Guided by this result, we studied three groups of EC-free electrolytes, which consisted of EMC and TG with $LiPF_6$ and LiTFSI. Although electrolytes with EMC and $LiPF_6$ exhibit fast capacity decay, both new electrolyte systems with LiTFSI show higher capacity and better stability than the EC-containing electrolytes in the electrochemical tests on Si electrodes. However, in contrast to the more stable EMC-based electrolyte, a continuous TG degradation in the TG-based electrolyte is observed particularly if the Si electrodes were completely lithiated down to 10 mV vs. Li.

While silicon anodes as lithium ion battery materials might require tailored electrolyte and binder systems optimized for silicon composition, surface and morphology, it is clear that a model-system approach is the most suitable way to achieve this optimization. This work explores and demonstrates a new and powerful model-compound based method to screen and study the potential electrolyte solvents specific to Si anodes in Li-ion batteries.

II. EXPERIMENTAL SECTION

II.A. Material Preparation.

LS with a Li:Si stoichiometry of 7:3 was synthesized from a stoichiometric mixture of the elements using pure Li (high purity alloy grade from Livent Corp.) and pure Si (325 mesh 99% purity from Sigma Aldrich). Smaller particle silicon was evaluated but had a higher percentage of passivating surface silica that carried thru as additional impurities to the reaction products. The mixture was first heated to 750 ^{o}C in a covered Ta container held for 1 h, then slowly cooled to 700 ^{o}C and quenched to room temperature. Freshly prepared LS was ground in an agate mortar and pestle for 5 min in the Ar glovebox (with O_2 and H_2O levels below 0.5 ppm) before mixing with different electrolyte solvents. The solvents, including EC, EMC, TG, and FEC, were all purchased from Sigma Aldrich. For reference, no physical changes were observed for the mortar and pestle after mixing LS with solvents. In comparison, when the fresh LS powder was filled into ZrO_2 NMR rotor, the part in direct contact with the fresh powder became blackish after the overnight experiment, demonstrating that the fresh LS is very reactive. [16]

II.B. Chemical and Structural Characterizations.

MAS-NMR experiments were performed at 7.02 T (300 MHz) on a Bruker Avance III HD spectrometer operating at a Larmor frequency of 44.21 MHz. ^{7}Li spectra were acquired with a rotor synchronized echo pulse sequence (90°-τ-180°-τ-acq), where $\tau = 1/\nu_r$. A $\pi/2$ pulse width of 2.5 μs was used with sufficiently long pulse recycle delays of 15 s. The spectra were referenced to 1 M LiCl aqueous solution at 0 ppm. ^{19}F spectra were also acquired with a rotor synchronized echo pulse sequence (90°-τ-180°-τ-acq), where $\tau = 1/\nu_r$. A $\pi/2$ pulse width of 2.5 μs was used with sufficiently long pulse recycle delays of 30 s. The spectra were referenced to hexafluorobenzene at 0 ppm. ^{29}Si spectra were acquired with a single pulse measurement, with sufficiently long pulse recycle delays of 1 s. The spectra were referenced to tetramethylsilane at 0 ppm. The $^{1}H \rightarrow {}^{13}C$ cross polarization spectra were acquired at 10kHz with 4ms contact time and 2s pulse delay. TMS was used as a reference at 0 ppm.

X-ray diffraction (XRD) were acquired using Bruker D8 Advance diffractometer equipped with Cu–Kα radiation source (λ = 1.5418 Å). The powders were packed onto the sample holders and sealed using the X-ray transparent Kapton tape inside of the glovebox. The XRD data were processed using Bruker DIFFRAC.SUITE EVA software.

Scanning electron microscopy (SEM) images were taken using a Hitachi S-4700-II microscope in the Center for Nanoscale Materials (CNM) of Argonne National Laboratory, with the operation voltage of 20 kV. The synthesized LS powders were directly sprayed onto the conductive carbon tape for the imaging.

II.C. Electrochemical Testing.

For this study 2032-type coin cells were used to test the electrochemical performance of Si electrodes. The graphite-free high-Si concentration electrodes (Si+LiPAA electrodes) were prepared by Argonne's Cell Analysis, Modeling and Prototyping (CAMP) Facility. Cu foil was used as the current collector and was laminated with a slurry containing 80 wt% commercial silicon powder, 10 wt% carbon additive (C45), and 10 wt% Lithium Polyacrylate (LiPAA) binder, mixed in distilled water. To deconvolute the reactions of binder material demonstrated previously,[32] from the electrolyte stability in contact with the lithiated Si, we also prepared binder-free loose-powder Si electrodes consisting 60 wt% Si and 40 wt% C45. In half-cell tests, the negative electrodes were Li metal and the positive electrodes were the Si electrodes (with or without binders). Various electrolytes were used in this paper, with their compositions listed in Table 1. Celgard-2325 was used as the separator.

Table 1. Receipts of electrolytes used in the electrochemical tests.

Notation	Components
Gen2	1.2 M $LiPF_6$ in a 3:7 mixture of EC and EMC
GenF	Gen2 electrolyte + 10 wt% FEC
TGLi	1 M LiTFSI in TG
TGLiF	TGLi electrolyte + 10 wt% FEC
EF	1 M LiTFSI in EMC+ 10 wt% FEC
EEF	1 M LiTFSI in a 3:7 mixture of EC and EMC + 10 wt% FEC
LE	1.2 M $LiPF_6$ in EMC
LEF	LE electrolyte + 10 wt% FEC

III. RESULTS AND DISCUSSIONS

LS model compound with the stoichiometry of Li_7Si_3 was synthesized to simulate the direct chemical interaction between electrolyte solvents and charged Si anodes. The stoichiometry was chosen as it represents the most thermally stable compound in the phase diagram therefore easy to handle, mimics the active electrode material near 300mV, and is capable of being either oxidized (to $Li_{12}Si_7$) or reduced to $Li_{13}Si_4$ to allow for various reaction mechanism options to be observed. The SEM images of as-made LS can be found in Figure S1. As reported previously, the XRD results of the pristine LS powder show that the LS powder also contains a small percentage of the $Li_{12}Si_7$ phase which probably arose due to Li loss

during the synthesis process.[16] In addition, it should be noted that although XRD is only sensitive to crystalline phases and actual lithiated species formed during the charging of Si anodes could be amorphous LS, [29, 33] previous solid-state NMR studies have shown that the local Li chemical environment in amorphous LS is comparable to those in the crystalline LS. [34, 35] Particularly, the Li_7Si_3 and $Li_{12}Si_7$ phases are similar to the LS formed after charging down to ~ 0.1 V vs. Li [34,36]. Therefore, pristine LS synthesized in this work is estimated to be a good model system to simulate the reactions of electrolyte solvents with intermediate-stage charged Si anodes.

To study the interactions between lithiated Si electrodes and different electrolyte solvents, pristine LS powders were soaked into FEC, EMC, and TG, respectively, with the volume ratio of 1:1. The mixtures were then packed into the ZrO_2 rotor for NMR measurements. In the case of EC, since it is solid at room temperature, the solid EC and LS powders were added into the NMR rotor consequently, and then heated up to 325 K inside the NMR probe under MAS to melt the EC and let it fully react with LS powders. The ^{7}Li NMR spectra of the initial LS + EC solid mixture at 298 K (room temperature), the mixture heated up to 325 K, and the mixture cooled back to 298 K can be found in Figure S2 in the SI. The effect of elevated temperature on reactivity and lithium NMR shifts are discussed in more detail in Supplemental Information. Compared with the pristine LS sample, a large positive change in chemical shift of 2 ppm can be found after mixing LS powders with solid EC, representing the loss of Li^+ from the bulk of LS structures consistent with the trends in ^{7}Li NMR signatures of Li_7Si_3 and $Li_{12}Si_7$ phases. [16, 34] This shows that the highly reductive LS is reactive enough to reduce solid EC and is delithiated through direct contact after simple mixing and MAS process (at 10kHz spinning, mixing is enhanced). After heating the heterogeneous mixture up to 325 K to melt the EC *in situ* and then cooling back to room temperature (298K), another change in shift of 0.4 ppm can be observed compared with the initial mixture of Li_7Si_3 and EC. This smaller shift after heat treatment implies that although melting the EC can further delithiate the Li_7Si_3 presumably by increasing the contacting surface area, most of the delithiation happens during the initial solid-solid contact between Li_7Si_3 and EC prior to or during the MAS operation. For the mixture of Li_7Si_3 and other liquid solvents, including EMC, FEC, and TG, smaller changes in chemical shifts in ^{7}Li NMR spectra (see Figure 1a) are observed compared with the EC mixture, which are +1.2, +0.5 and +0.1 ppm, respectively. Based on the lithium environment data of all the tested solvents in contact with Li_7Si_3, EC was found to be the most reactive. ^{29}Si NMR results shown in Figure 1b are also consistent with these findings, where the mixture of Li_7Si_3 and EC demonstrates the largest Si chemical shift change (+12.5 ppm) among all the Li_7Si_3-solvent mixtures compared with the pristine Li_7Si_3. The reaction between Li_7Si_3 and EC suggests any contact between EC and freshly generated lithiated silicon in a Si anode can cause severe side reactions as well as formation of silicon dimers and clusters, even at early charging stages, which were observed in previous studies. [16, 29, 30, 31]. Meanwhile, other solvents lead

to smaller chemical shifts in ^{7}Li and ^{29}Si NMR after mixing with Li_7Si_3, implying they have better chemical stability and therefore better stability in contact with the charged Si anode. Particularly, for the mixing of Li_7Si_3 with TG, there is almost no shift in ^{7}Li NMR peak position compared with the pristine Li_7Si_3, however a clear broadening can be found in the mixture. This means soaking Li_7Si_3 in TG may not be causing severe delithiation, as with EC and EMC, but trace lithium loss can result in distribution of different lithium local environments resulting in a broader lithium peak. This is also consistent with the notable chemical shift of the Li_7Si_3 + TG mixture in the ^{29}Si NMR spectrum compared with the pristine Li_7Si_3 (see Figure 1b).

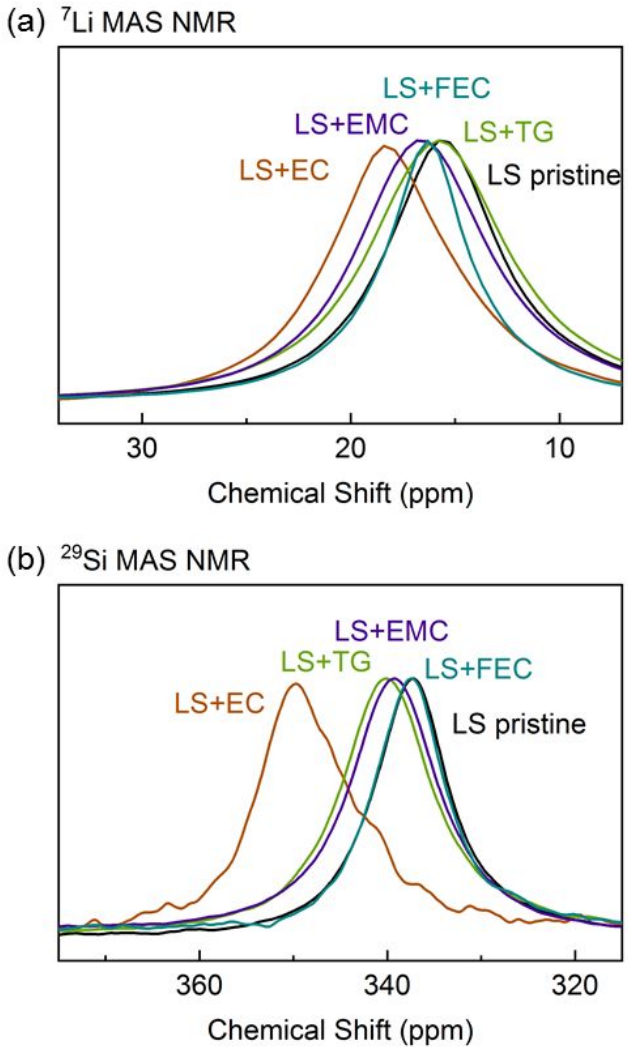

Figure 1. (a) ^{7}Li and (b) ^{29}Si MAS NMR spectra of pristine LS model compound and its mixtures with TG, FEC, EMC, and EC, respectively, with the volume ratio of 1:1. The spectra were acquired at 10

kHz using a 3.2 mm MAS probe at 298 K. The mixture of LS+EC was heated up to 325 K and then cooled back to 298 K.

It must be noted that this study mostly focuses on reactivity of lithium silicides (as model system) only with different solvents, where the effect of different salts on solvation is not studied in detail. However, our initial studies on LS reaction with Gen2 electrolyte system also shows similar ^{7}Li NMR shift behavior with EC solvent, suggesting the changes are mostly due to solvent structure (Figure S3).

These changes observed in NMR peak positions are directly correlated with the chemical reactivity of the solvent and lithiated silicon. $Si^{-2/-4}$ anions in Li-Si Zintl phases are highly reactive and can act as pseudo-nucleophiles attacking electrophilic sites in organic solvent molecules forming electrolyte decomposition products in SEI. Possible electrochemical decomposition reactions of common solvents such as EC, EMC and FEC have been covered in different studies [16, 28, 29, 30] suggesting; FEC is reduced through the opening of the five-membered ring leading to the formation of lithium poly (vinyl carbonate), LiF, and dimers all via electrochemical processes. Linear carbonates, such as EMC, are electrochemically more stable than cyclic carbonates due to lack of steric effects in closed membered rings. The reductive decomposition of linear carbonates is a stepwise reaction consisting first reductive formation of $^{-}COO\text{-}R_1$ and $^{\cdot}R_2$ followed by hydrogen abstraction and radical annihilation.[37]

In this study, we focus and emphasize the chemical reaction of the solvent molecule with the highly reactive silicon in the absence electrochemical reaction starts, *i.e* before an electron is supplied to reduce the organic molecule. Instead, the electron is supplied by the oxidation reaction of the Zintl phase. Possible reactions of EC with silicon anions was shown in our previous report [16] as given in Schemes 1 and 2;

Scheme 1. Proposed electron formation reaction

$$[Si\text{-}Si]^{-4} \longrightarrow 2[Si]^{-2}$$

$$[Si]^{-2} \longrightarrow 2\,\delta e^{-} + [Si]^{2\delta-2}$$

Scheme 2. Proposed reaction for EC

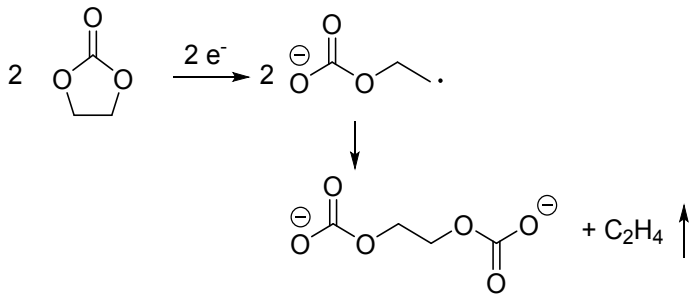

Based on similar spectroscopic observations after reacting with lithiated silicon, the reduction of FEC can be summarized below in Scheme 3; [37-39]

Scheme 3. Proposed reaction for FEC

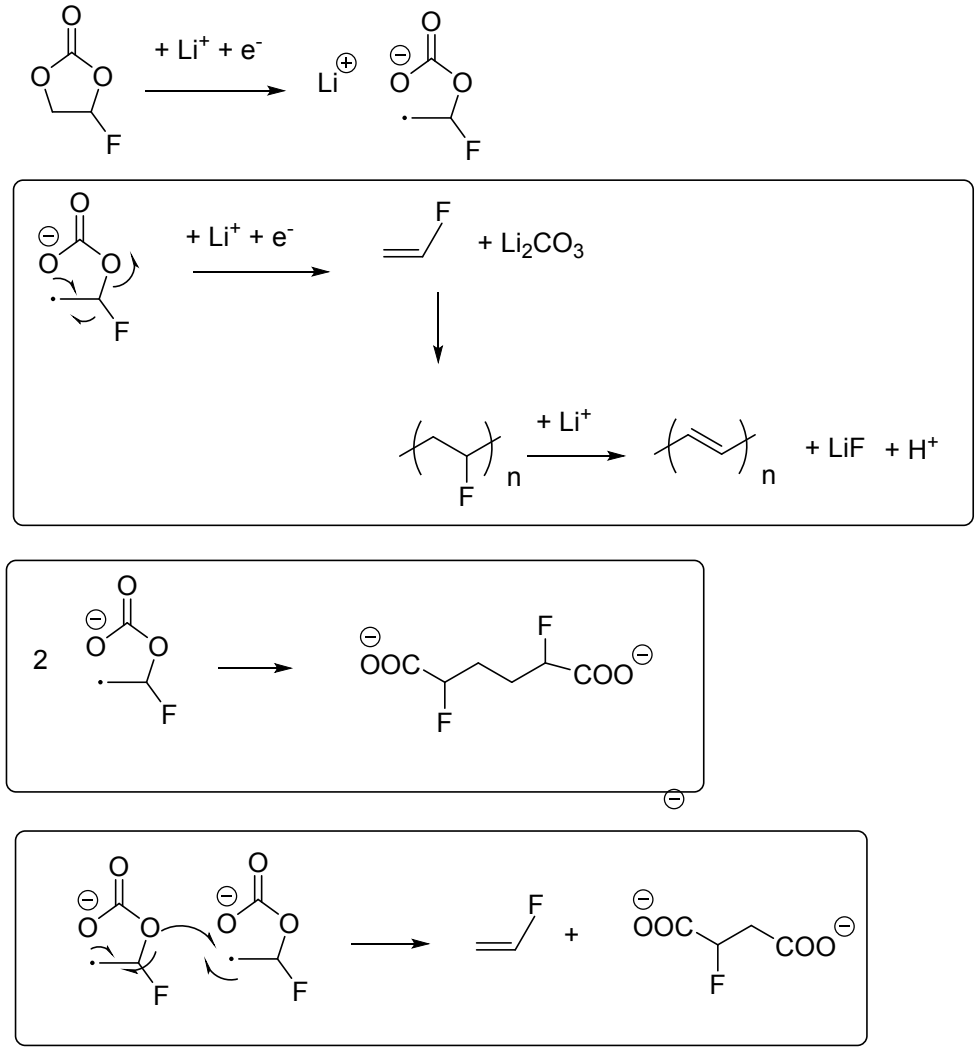

On the other hand, TG exhibits higher cathodic stability towards the energized electrode surface: the decomposition pathway mostly involves breakdown the R. and .O-$(CH_2CH_2-O)_3$-CH_3 (Scheme 4). Despite the direct chemical stability of TG, stable SEI formers (such as LiF, Li_2CO_3 in inner layer, semi-carbonates and PEO oligomers in outer layer etc.) for TG is explored in electrochemical tests below for long-term electrochemical kinetic stability of TG.

Scheme 4. Proposed reaction for TG

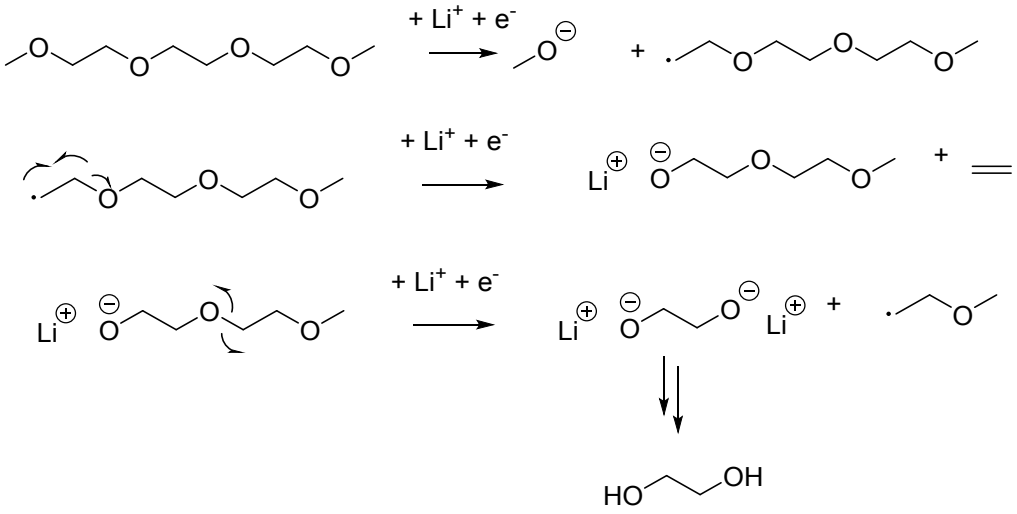

The reaction products of FEC and model sample Li_7Si_3 were studied by ^7Li and ^{19}F solid state NMR. As seen in Figure 2a with ^7Li NMR, with the reaction of Li_7Si_3 phase and FEC the lithium peaks slightly shift to higher frequencies due to lithium loss consisttent with previous studies.[8] Formation of LiF is also observed both by ^7Li and ^{19}F NMR which suggests that the salt formation happens even at early stages of charging of the silicon anodes. The additional peaks observed with ^7Li NMR data after FEC interaction are due to lithium bearing decomposition products and $Li_{12}Si_7$ (which is also seen in the pristine sample and is due to synthesis impurities). ^{19}F NMR of model Li_7Si_3 and FEC mixture shows peaks for FEC and LiF mainly. The broad peak at around -240 ppm can be due to fluorine atoms in saturated and unsaturated aliphatic compounds shown in scheme 3 for FEC decomposition.

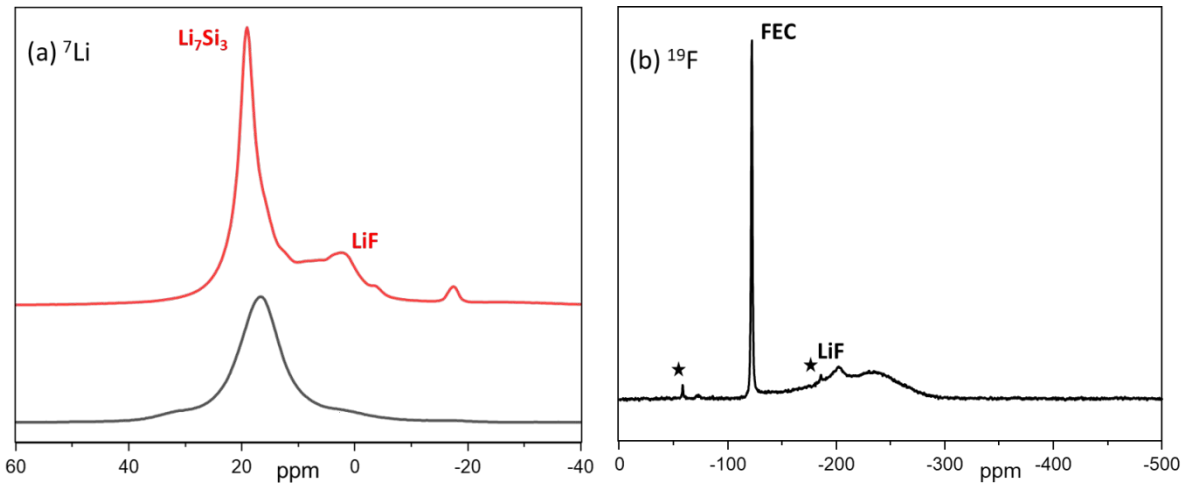

Figure 2. (a) ^7Li MAS NMR spectra of pristine Li_7Si_3 (black) and its mixtures with FEC (red) (b) ^{19}F MAS NMR spectra of Li_7Si_3 with FEC

According to the above NMR results it is shown that EC is far more reactive than TG, EMC (or a shorter chain linear carbonate DMC, see Figure S4), and FEC in contact with lithiated Si, and Si^{-4} anions formed are too reactive with any species they come in contact with. Therefore, a tailored electrolyte approach is crucial for silicon anode systems, where solvent, binders or salts that are prone to nucleophilic are minimized or not used at all. For example, if the electrolyte formulation with EC is non-passivating the silicon electrode surface under electrochemical conditions, it is crucial to develop EC-free electrolytes or reduce EC content, to minimize side reactions that will occur while new lithium silicide surfaces are generated with cycling.

Previous studies on traditional graphite batteries have shown that EC is key in forming a stable SEI and preventing the destruction of the layered structure of graphite electrodes[40]. To have a functional EC-free electrolyte, the anode needs to be graphite free, such as a graphite-free Si-only anode. To test the electrochemical reactivity and performance of EC-free electrolyte formulations in contact with the lithiated Si electrodes, we performed electrochemical tests on both EC containing (i.e. Gen2, GenF and EEF) and EC-free electrolyte systems (including the TG-based electrolytes TGLi and TGLiF, and the EMC-based electrolytes EF, LE, and LEF in this work). TG-based electrolyte was tested first as TG led the smallest change in ^{7}Li MAS NMR chemical shifts after reacting with LS model compounds. Half-cell electrochemical tests were first performed on binder-free and graphite-free drop cast loose-powder Si electrodes, cycling between 1.5 and 0.01 V vs. Li first at C/20 for 3 formation cycles, then at C/3 for 7 aging cycles. As shown in Figure 3, in comparison with the commonly used Gen2 electrolyte with EC and EMC, using carbonate-free TG-based electrolytes (TGLi and TGLiF) can effectively increase the capacity of the Si electrodes by eliminating side reactions, particularly for the initial cycles. This is consistent with our NMR observations showing that the TG is less reactive in contact with LS than EC, therefore more Li can be inserted in and extracted out from the Si electrodes and less Li is lost during the initial cycles. However, TG was not found to be totally inert during the Si (de)lithiation process at least for the electrochemical windows selected. As shown in the insert plot in Figure 3a, with TGLi electrolyte, an additional reducing plateau at ~0.45 V can be found in the first lithiation process. This plateau could be related to the degradation of TG during the initial SEI formation process via electrochemical reactions. A similar behavior was also observed in a study on Li-ion half cells with Si with a LiTFSI/TG electrolyte by Wu et al [41]. This plateau disappears in the second lithiation cycle, as shown in the inserts in Figures 3b and 3c, indicating the reaction with TG is greatly suppressed after the initial SEI forms. Gen2 and TGLi electrolytes show similar coulombic efficiency of ~90% over the C/3 aging cycles, indicating similar lithium loss caused by the SEI formation and side reactions. To further stabilize the electrolyte and SEI layer during the charging/discharging process, FEC was added to have GenF and TGLiF electrolytes.

After adding FEC, both Gen2 and TGLi systems show much improved coulombic efficiencies of ~95% during the C/3 aging cycles, implying that FEC can be used to stabilize the SEI formation in both EC-based and TG-based electrolytes. Adding FEC to TGLi electrolyte also suppressed the reducing platform at ~0.45 V in the first lithiation cycle (see the inset of Figure 3a), which also indicates that FEC can help to reduce the potential degradation of TG and therefore stabilize the SEI formation in TG-based electrolyte. Despite the similar coulombic efficiencies between EC-based and TG-based electrolytes (with or without FEC additives), faster capacity losses can be observed when using TG-based electrolyte (TGLi or TGLiF), as shown in Figures 3d and 3e. During the 7 aging cycles, TG-based electrolyte led to capacity losses of ~40%, while the capacity losses are only ~25% for Gen2 and ~5% for GenF electrolytes.

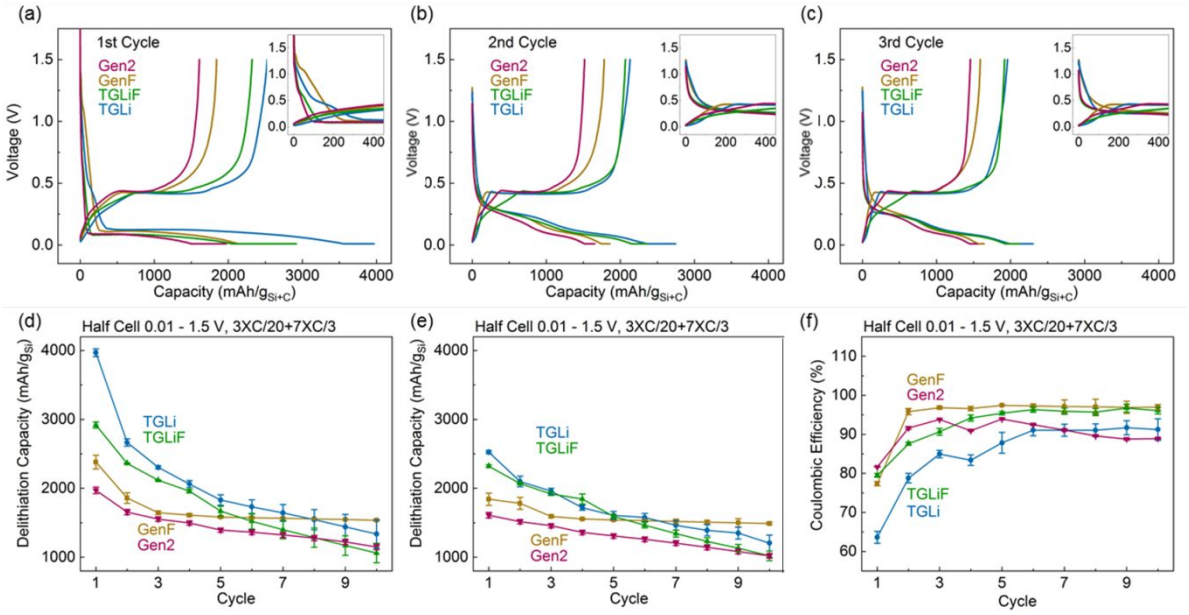

Figure 3. Half-cell loose-powder electrochemical test results, with the Si:C mass ratio of 3:2. The Gen2 and TGLi electrolytes as well as their mixing with 10% FEC as the additive were used in the electrochemical tests. The charge and discharge curves of the 1st, 2nd, and 3rd cycles are shown in panels (a)-(c), respectively. The inserts are the zoom-ins of the initial charging/discharging stages. The lithiation and delithiation capacities as well as the coulombic efficiencies over cycles are shown in panels (d)-(f). The capacities are normalized by the mass of silicon. The cells were cycled from 0.01 to 1.5 V, first at the rate of C/20 for 3 formation cycles, then at the rate of C/3 for 7 aging cycles. The cells were held at 0.01 V until the current is below C/100 at the end of each lithiation process to accelerate the aging effect. Error bars represent the standard deviation of at least three measurements for each sample.

To explore the influence of the lithiation degree of Si electrodes on the stability of electrolyte, we changed the lithiation voltage from 0.01 to 0.05 V to reduce the total amount of lithium insertion into the loose-powder Si electrodes. As shown in Figure S6 in the SI, under the milder lithiation process down to 0.05 V, the TGLi electrolyte shows much higher capacity retention (~80%) over 7 aging cycles with much higher coulombic efficiencies (~98.5%) for each aging cycle, which performs much better than the 0.01 V TGLi case and similarly to the 0.05 V GenF case. After electrochemical aging with TGLi electrolyte at different voltage ranges, the Si electrodes (having been delithiated at 1.5 V) were taken out and rinsed by dimethyl carbonate (DMC) gently, then the loose powders on the Cu foil were scratched down for NMR characterizations. As shown in the ^{7}Li NMR spectra in Figure 4a, a lower cut-off voltage of 0.01 V for the Si electrode lithiation process leads to the formation of a new ^{7}Li peak at ~10 ppm compared with that lithiated down to 0.05 V, which represents low-Li concentration LS. This means when the lithiation voltage is down to 0.01 V, more Li_xSi was left (i.e. more Li was trapped) in the Si electrode after 10 cycles (ended with delithiation up to 1.5 V) compared with that lithiated down to 0.05 V. This is consistent with the electrochemical test observations on Si half cells cycled in TGLi electrolyte down to 0.01 V which caused more capacity loss and lower coulombic efficiencies than that cycled down to 0.05 V. ^{1}H/^{13}C Cross Polarization NMR (Figure 4b) demonstrate that the reaction between TG and lithiated Si electrodes decomposes TG into ethylene glycol, methanol, and other small organic compounds. This shows, although TG shows better stability than EC in contact with Li_7S_3 in NMR measurements, in real applications, TG will still degrade in contact with Si electrodes lithiated down to practical voltages.

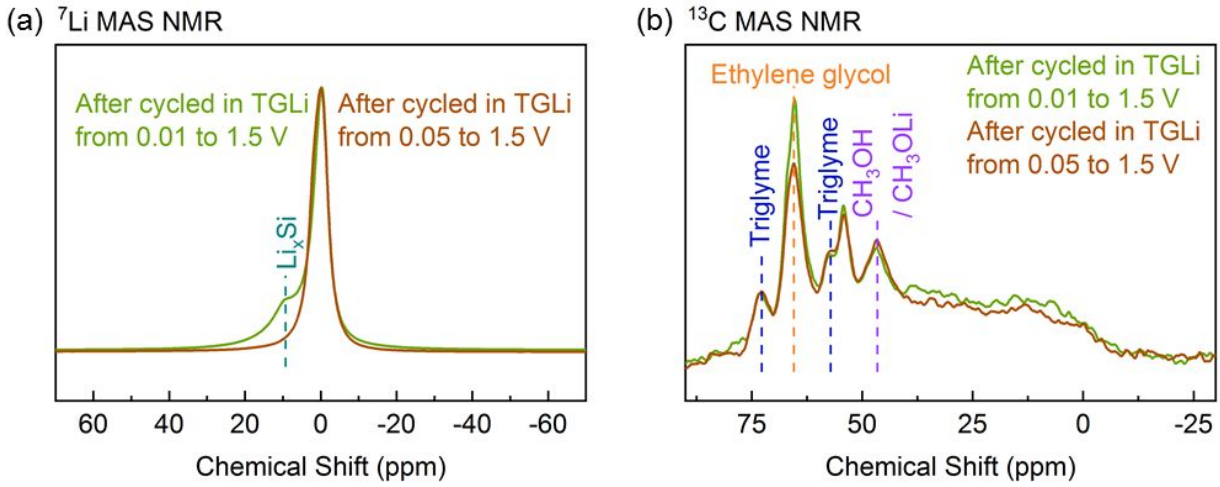

Figure 4. (a) ^{7}Li and (b) ^{1}H-coupled ^{13}C MAS NMR spectra of Si loose powders after cycling between either 0.01 to 1.5 V or 0.05 to 1.5V for 10 cycles in the TGLi electrolyte. The spectra were acquired at 65 and 20 kHz, respectively, using a 1.3 mm MAS probe.

In addition to adding FEC in the electrolyte, another way to mitigate the continuous SEI formation on Si electrode over cycles is to constrain the Si powders using strong binder materials[16-19]. With the help from Argonne's Cell Analysis, Modeling and Prototyping (CAMP) facility, we were able to make large-scale graphite-free Si laminations with 80 wt% high Si concentration and 10 wt% LiPAA binders, which could provide more accurate and reproducible electrochemical measurements on the influence of different electrolytes. Using these high-Si-concentration electrodes with LiPAA binders, we re-measured the half-cell electrochemical performance using different electrolytes. As shown in Figure 5, similar to the loose-powder electrodes, the Si+LiPAA electrodes also show much higher initial capacity in TG-based electrolytes (TGLi and TGLiF) than in EC-based electrolytes (Gen2 and GenF), demonstrating, that the less reactive TG solvent enables more Li insertion/extraction during the charging/discharging processes. At the same time, compared with the loose-powder electrodes, adding binders and reducing carbon concentrations in Si+LiPAA electrodes lead to worse ionic and electric conductivities. As the results show, higher capacity drops between the last C/20 formation cycle and the first C/3 aging cycle can be observed on Si+LiPAA electrodes than on loose-powder Si electrodes no matter which electrolyte was used, implying a higher impedance and a worse rate performance. The additional plateau observed at ~0.45 V in loose-powder measurements (Figure 3a) during the first lithiation in TG-based electrolytes disappeared in Si+LiPAA cases (Figure 5a), indicating the LiPAA binder could further reduce the side reaction of TG degradation particularly during the initial lithiation process. As shown in Figures 5d and 5e, the electrochemical data with TGLiF electrolyte demonstrates almost twice the lithiation/delithiation capacity with higher capacity retention during the aging cycling (65% over 7 cycles) compared with the GenF electrolyte (46% over 7 cycles) on Si+LiPAA electrodes.

Here we further extended the C/3 aging cycling to 100 cycles, as shown in Figure S6. After 100 C/3 cycles, the Si+LiPAA electrode still shows a high delithiation capacity of 188 mAh/g_{Si} with the coulombic efficiency of 99.5% in TGLiF electrolyte, much better than the GenF electrolyte with the delithiation capacity of 84 mAh/g_{Si} with the coulombic efficiency of 98.6%. On the other hand, the TGLi electrolyte shows similarly high capacity to the TGLiF electrolyte during the initial C/20 formation cycles, however its capacity drops much faster during the C/3 cycling (33% capacity retention over 7 aging cycles), and the coulombic efficiency jumps higher than 100% after 12 cycles (see Figure S6c), indicating severe TG degradation during long cycling. This means compared with the loose-powder Si electrodes, on Si+LiPAA electrodes with higher Si concentrations, the stabilization effect of FEC becomes more critical for the TG-based electrolytes.

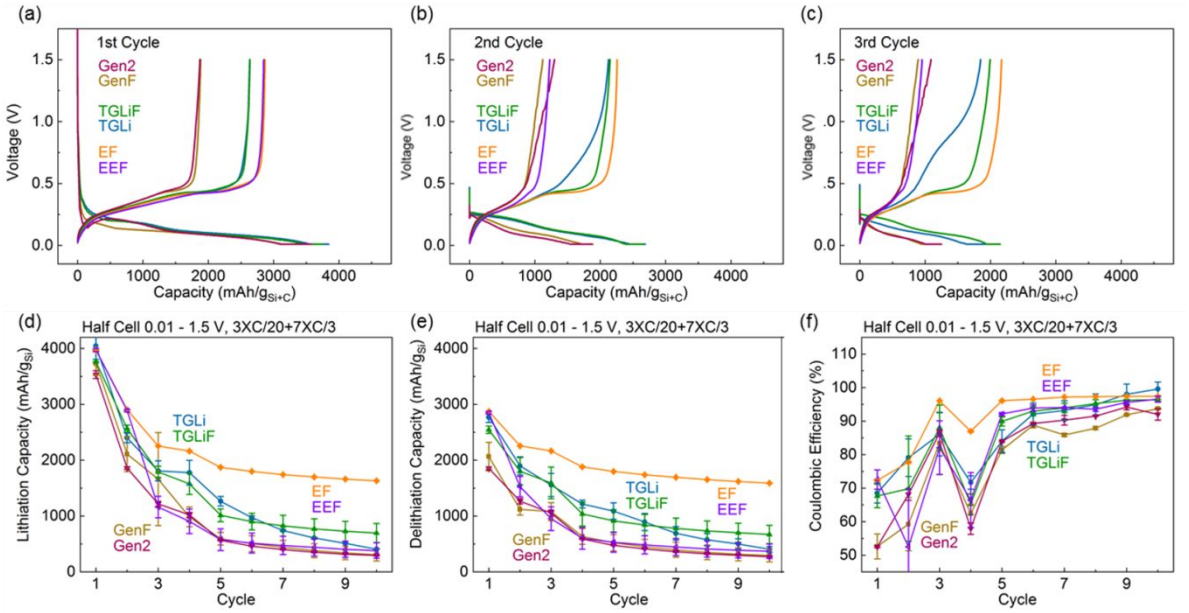

Figure 5. Half-cell electrochemical test results on Si+LiPAA electrodes. Gen2, GenF, TGLi, TGLiF, EF, and EEF were used in the electrochemical tests. The charge and discharge curves of the 1st, 2nd, and 3rd cycles are shown in panels (a)-(c), respectively. The lithiation and delithiation capacities as well as the coulombic efficiencies over cycles are shown in panels (d)-(f). The capacities are normalized by the mass of silicon and carbon additive. The cells were cycled from 0.01 to 1.5 V, first at the rate of C/20 for 3 formation cycles, then at the rate of C/3 for 7 aging cycles. The cells were held at 0.01 V until the current is below C/100 at the end of each lithiation process to accelerate the aging effect. Error bars represents the standard deviation of at least three measurements for each sample.

In addition to TG-based electrolytes, we also tried EMC-based EC-free electrolyte, EF, which contains only EMC and FEC as the solvent. LiTFSI is used as the salt in EF electrolyte and $LiPF_6$ is used in LE/LEF electrolytes, to make a good comparison with TG-based electrolyte. To test the potential influence of changing the salt from $LiPF_6$ to LiTFSI, we also prepared a new baseline electrolyte EEF (LiTFSI dissolved in EC, EMC, and FEC) to compare with the traditional $LiPF_6$-based GenF electrolyte. The half-cell results of LE and LEF electrolytes are shown in Figure S6. Interestingly, the cells with LE electrolyte exhibit extremely fast capacity fading in the initial cycles and could not operate over 5 cycles. Cells with LEF electrolyte are slightly better but the capacity drops to zero within ten cycles. The results clearly indicate that LE and LEF are not viable electrolytes for Si anodes. It is probably because of the incompatibility between $LiPF_6$ and EMC, which is reflected by the fact that $LiPF_6$ was hard to dissolve into EMC even with FEC additive. The half-cell results of EF and EEF electrolytes on Si+LiPAA

electrodes are shown in Figure 5. Comparison of EEF with GenF shows that, after changing the salt from $LiPF_6$ to LiTFSI, significantly higher delithiation capacity as well as higher efficiency can be obtained during the first cycle. However, starting from the second cycle, the capacity and efficiency of the cells with EEF electrolyte quickly drop and show similar electrochemical performance with the cells prepared with GenF or Gen2 electrolyte. This shows that comparing with $LiPF_6$, LiTFSI can provide better initial performance, but quickly with the second cycle, the instability of EC leads to similar poor performance among all EC-containing electrolytes (EEF, Gen2 and GenF). On the other hand, the EF electrolyte shows similar performance to EEF in the first cycle, however due to its EC-free chemistry, the improved initial capacity and performance can be well maintained over the extended cycles. The cyclability of EF electrolyte is even better than the TG-based electrolyte.

These studies prove that, EC is the main source of chemical instability in cells with Si electrodes, that use traditional lithium-ion battery electrolytes, which is consistent with our model study results. Although, TG showed slightly better stability than EMC in the model compound study, it cannot effectively passivate the lithiated Si electrodes in electrochemical tests likely due to a poor SEI, therefore the TG-based EC-free electrolytes demonstrate poor capacity retention rates and lower coulombic efficiencies than the EMC-based EC-free electrolytes. This indicates that the chemical stability alone is not sufficient to predict the long-term cyclability of the electrolyte solvents in the application of Si electrodes. While FEC addition aids in inorganic SEI formation (LiF), the nature of the organic and inorganic SEI depends highly on the solvent choice and it is clear none of the tested solvent systems (general or specific) in this study was capable of providing a stable and passivating SEI.

IV. CONCLUSIONS

In this work, we use lithium silicide model compounds to simulate the potential reactions between lithiated Si anodes and commonly used electrolytes. From the NMR results, we find that EC in traditional electrolytes is the most reactive solvent among all the tested solvents in contact with the LS model compounds, indicating chemical instability. Unless proven to be perfectly passivating on the surface, in a system where reactive active material surfaces are continuously generated, it can be speculated that the use of EC should be avoided and/or minimized in silicon specific electrolyte formulations. In comparison, EMC, TG and FEC show less interaction after mixed with LS powders. Guided by these results, we studied several new EC-free electrolytes, which can provide higher capacity with better capacity retention rates in half-cell tests on graphite-free Si anodes. However, even with the most inert solvents, electrophilic centers undergo attack from silicon anions. It is clear that the fields focus should shift to other and perhaps more suitable electrolyte systems to be tailored specifically for silicon anodes, in the future that will primarily alleviate this reaction and/or passivate the surface to stop the unwanted reactions going on indefinitely and reducing efficiencies. Therefore, the mitigation of capacity fade and silicon electrode failure requires understanding of when and how the decomposition products aid in the formation of an effectively passivating surface layer. Still we demonstrate that it is crucial to study solvent-silicon reactivity and find the optimum electrolyte system specific for silicon anodes. The model-compound based method applied in this study provides a systematic and well-controlled approach to examine the electrode-electrolyte interaction and SEI formation processes on Si electrodes, as well as new electrolyte systems that could be used in future Si-electrode Li-ion batteries.

ASSOCIATED CONTENT

Supporting Information

The Supporting Information is available free of charge on the Publications website.

Author Information

Corresponding Author

*Email: hbhtiancai@gmail.com, fdogan@anl.gov, bkey@anl.gov

Notes

The authors declare no competing financial interest.

ACKNOWLEDGEMENT

Support from the Vehicle Technologies Program, at the U.S. Department of Energy, Office of Energy Efficiency and Renewable Energy are gratefully acknowledged. The submitted manuscript has been created by UChicago Argonne, LLC, Operator of Argonne National Laboratory ("Argonne"). Argonne, a U.S. Department of Energy Office of Science laboratory, is operated under Contract No. DE-AC02-06CH11357. This work used SEM from the Center for Nanoscale Materials at Argonne, which are supported by the U. S. Department of Energy, Office of Science, Office of Basic Energy Sciences, also under Contract No. DE-AC02-06CH11357.

REFERENCES

(1) Kasavajjula, U.; Wang, C.; Appleby, A. J. Nano- and Bulk-silicon-based Insertion Anodes for Lithium-ion Secondary Cells, *J. Power Sources* 2007, 163, 1003–1039.

(2) Maranchi, J. P.; Hepp, A. F.; Kumta, P. N. High Capacity, Reversible Silicon Thin-Film Anodes for Lithium-Ion Batteries, *Electrochem. Solid-State Lett.* 2003, 6, A198–A201.

(3) Winter, M.; Besenhard, J. O.; Spahr, M. E.; Novák, P. Insertion Electrode Materials for Rechargeable Lithium Batteries, *Adv. Mater.* 1998, 10, 725–763.

(4) Wu, H.; Cui, Y. Designing Nanostructured Si Anodes for High Energy Lithium Ion Batteries, *Nano Today* 2012, 7, 414–429.

(5) Nesper, R. Structure and Chemical Bonding in Zintl-phases Containing Lithium, *Prog. Solid State Chem.* 1990, 20, 1–45.

(6) Nesper, R.; Von Schnering, H. G. $Li_{21}Si_5$, a Zintl Phase as well as a Hume-Rothery Phase, *J. Solid State Chem.* 1987, 70, 48–57.

(7) Nesper, R.; Von Schnering, H. G.; Curda, J. $Li_{12}Si_7$, eine Verbindung mit trigonal-planaren Si4 ‐ Clustern und isometrischen Si5-Ringen, *Chem. Ber.* 1986, 119, 3576–3590.

(8) Key, B.; Morcrette, M.; Tarascon, J. M.; Grey, C. P. Pair Distribution Function Analysis and Solid State NMR Studies of Silicon Electrodes for Lithium Ion Batteries: Understanding the (De)lithiation Mechanisms, *J. Am. Chem. Soc.* 2011, 133, 503–512.

(9) Key, B.; Bhattacharyya, R.; Morcrette, M.; Seznec, V.; Tarascon, J. M.; Grey, C. P. Real-Time NMR Investigations of Structural Changes in Silicon Electrodes for Lithium-Ion Batteries, *J. Am. Chem. Soc.* 2009, 131, 9239–9249.

(10) Yoshio, M.; Wang, H.; Fukuda, K.; Umeno, T.; Dimov, N.; Ogumi, Z. Carbon-Coated Si as a Lithium-Ion Battery Anode Material, *J. Electrochem. Soc.* 2002, 149, A1598–A1603.

(11) Hatchard, T. D.; Dahn, J. R. In Situ XRD and Electrochemical Study of the Reaction of Lithium with Amorphous Silicon, *J. Electrochem. Soc.* 2004, 151, A838–A842.

(12) Winter, M.; Besenhard, J. O. Electrochemical Lithiation of Tin and Tin-based Intermetallics and Composites, *Electrochim. Acta* 1999, 45, 31–50.

(13) Ma, D.; Cao, Z.; Hu, A. Si-Based Anode Materials for Li-Ion Batteries: A Mini Review, *Nanomicro. Lett.* 2014, 6, 347–358.
(14) Su, X.; Wu, Q.; Li, J.; Xiao, X.; Lott, A.; Lu, W.; Sheldon Brian, W.; Wu, J. Silicon‐Based Nanomaterials for Lithium‐Ion Batteries: A Review, *Adv. Energy Mater.* 2013, 4, 1300882.
(15) Nitta, N.; Wu, F.; Lee, J. T.; Yushin, G. Li-ion Battery Materials: Present and Future, *Mater. Today* 2015, 18, 252–264.
(16) Han, B.; Liao, C.; Dogan, F.; Trask, S. E.; Lapidus, S. H.; Vaughey, J. T.; Key, B. Using Mixed Salt Electrolytes to Stabilize Silicon Anodes for Lithium-Ion Batteries via in Situ Formation of Li–M–Si Ternaries (M = Mg, Zn, Al, Ca), *ACS Appl. Mater. Interfaces* 2019, 11, 29780–29790.
(17) Hochgatterer, N. S.; Schweiger, M. R.; Koller, S.; Raimann, P. R.; Wöhrle, T.; Wurm, C.; Winter, M. Silicon/Graphite Composite Electrodes for High-Capacity Anodes: Influence of Binder Chemistry on Cycling Stability, *Electrochem. Solid-State Lett.* 2008, 11, A76–A80.
(18) Kim, J. S.; Choi, W.; Cho, K. Y.; Byun, D.; Lim, J.; Lee, J. K. Effect of Polyimide Binder on Electrochemical Characteristics of Surface-modified Silicon Anode for Lithium Ion Batteries, *J. Power Sources* 2013, 244, 521–526.
(19) Koo, B.; Kim, H.; Cho, Y.; Lee, K. T.; Choi, N.-S.; Cho, J. A Highly Cross‐Linked Polymeric Binder for High‐Performance Silicon Negative Electrodes in Lithium Ion Batteries, *Angew. Chem.* 2012, 124, 8892–8897.
(20) Magasinski, A.; Zdyrko, B.; Kovalenko, I.; Hertzberg, B.; Burtovyy, R.; Huebner, C. F.; Fuller, T. F.; Luzinov, I.; Yushin, G. Toward Efficient Binders for Li-Ion Battery Si-Based Anodes: Polyacrylic Acid, *ACS Appl. Mater. Interfaces* 2010, 2, 3004–3010.
(21) Dalavi, S.; Guduru, P.; Lucht, B. L. Performance Enhancing Electrolyte Additives for Lithium Ion Batteries with Silicon Anodes, *J. Electrochem. Soc.* 2012, 159, A642–A646.
(22) Markevich, E.; Salitra, G.; Aurbach, D. Fluoroethylene Carbonate as an Important Component for the Formation of an Effective Solid Electrolyte Interphase on Anodes and Cathodes for Advanced Li-Ion Batteries, *ACS Energy Lett.* 2017, 2, 1337–1345.
(23) Etacheri, V.; Haik, O.; Goffer, Y.; Roberts, G. A.; Stefan, I. C.; Fasching, R.; Aurbach, D. Effect of Fluoroethylene Carbonate (FEC) on the Performance and Surface Chemistry of Si-Nanowire Li-Ion Battery Anodes, *Langmuir* 2012, 28, 965–976.
(24) Choi, N.-S.; Yew, K. H.; Kim, H.; Kim, S.-S.; Choi, W.-U. Surface Layer Formed on Silicon Thin-film Electrode in Lithium Bis(oxalato) Borate-based Electrolyte, *J. Power Sources* 2007, 172, 404–409.
(25) Han, G.-B.; Ryou, M.-H.; Cho, K. Y.; Lee, Y. M.; Park, J.-K. Effect of Succinic Anhydride as an Electrolyte Additive on Electrochemical Characteristics of Silicon Thin-film Electrode, *J. Power Sources* 2010, 195, 3709–3714.
(26) Chen, L.; Wang, K.; Xie, X.; Xie, J. Effect of Vinylene Carbonate (VC) as Electrolyte Additive on Electrochemical Performance of Si Film Anode for Lithium Ion Batteries, *J. Power Sources* 2007, 174, 538–543.
(27) Ma, L.; Glazier, S. L.; Petibon, R.; Xia, J.; Peters, J. M.; Liu, Q.; Allen, J.; Doig, R. N. C.; Dahn, J. R. A Guide to Ethylene Carbonate-Free Electrolyte Making for Li-Ion Cells, *J. Electrochem. Soc.* 2017, 164, A5008–A5018.

(28) Bridel, J.-S.; Grugeon, S.; Laruelle, S.; Hassoun, J.; Reale, P.; Scrosati, B.; Tarascon, J.-M. Decomposition of Ethylene Carbonate on Electrodeposited Metal Thin Film Anode, *J. Power Sources* 2010, 195, 2036 –2043.

(29) Jin, Y.; Kneusels, N. H.; Magusin, P. C. M. M.; Kim, G.; Castillo-Martinez, E.; Marbella, L. E.; Kerber, R. N.; Howe, D. J.; Paul, S.; Liu, T.; Grey, C. P. Identifying the Structural Basis for the Increased Stability of the Solid Electrolyte Interphase Formed on Silicon with the Additive Fluoroethylene Carbonate, *J. Am. Chem. Soc.* 2017, 139, 14992–15004.

(30) Michan, A. L.; Leskes, M.; Grey, C. P. Voltage Dependent Solid Electrolyte Interphase Formation in Silicon Electrodes: Monitoring the Formation of Organic Decomposition Products, *Chem. Mater.* 2016, 28, 385–398.

(31) Chen, X.; Li, X.; Mei, D.; Feng, J.; Hu, M. Y.; Hu, J.; Engelhard, M.; Zheng, J.; Xu, W.; Xiao, J.; Liu, J.; Zhang, J. G. Reduction Mechanism of Fluoroethylene Carbonate for Stable Solid–Electrolyte Interphase Film on Silicon Anode, *Chem Sus Chem* 2014, 7, 549–554.

(32) Han, B.; Piernas-Muñoz, M. J.; Dogan, F.; Kubal, J.; Trask, S. E.; Bloom, I. D.; Vaughey, J. T.; Key, B. Probing the Reaction between PVDF and LiPAA vs Li7Si3: Investigation of Binder Stability for Si Anode, *J. Electrochem. Soc.* 2019, 166, A2396–A2402.

(33) Antartis, D.; Dillon, S.; Chasiotis, I. Effect of Porosity on Electrochemical and Mechanical Properties of Composite Li-ion Anodes, *J. Compos. Mater.* 2015, 49, 1849–1862.

(34) Key, B.; Bhattacharyya, R.; Morcrette, M.; Seznéc, V.; Tarascon, J.-M.; Grey, C. P. Real-Time NMR Investigations of Structural Changes in Silicon Electrodes for Lithium-Ion Batteries, *J. Am. Chem. Soc.* 2009, 131, 9239–9249.

(35) Key, B.; Morcrette, M.; Tarascon, J.-M.; Grey, C. P. Pair Distribution Function Analysis and Solid State NMR Studies of Silicon Electrodes for Lithium Ion Batteries: Understanding the (De)lithiation Mechanisms, *J. Am. Chem. Soc.* 2011, 133, 503–512.

(36) Trill, J.-H.; Tao, C.; Winter, M.; Passerini, S.; Eckert, H. NMR Investigations on the Lithiation and Delithiation of Nanosilicon-based Anodes for Li-ion batteries, *J. Solid State Chem.* 2011, 15, 349–356.

(37) Seo, D. M.; Chalasani, D.; Parimalam, B. S.; Kadam, R.; Nie, M.; Lucht, B. L. Reduction Reactions of Carbonate Solvents for Lithium Ion Batteries, *ECS Electrochem. Lett.* 2014, 3, A91–A93.

(38) Markevich, E.; Salitra, G.; Aurbach, D. Fluoroethylene Carbonate as an Important Component for the Formation of an Effective Solid Electrolyte Interphase on Anodes and Cathodes for Advanced Li-Ion Batteries, *ACS Energy Lett.* 2017, 2, 1337–1345.

(39) Shkrob, I. A.; Zhu, Y.; Marin, T. W.; Abraham, D. Reduction of Carbonate Electrolytes and the Formation of Solid-Electrolyte Interface (SEI) in Lithium-Ion Batteries. 1. Spectroscopic Observations of Radical Intermediates Generated in One-Electron Reduction of Carbonates, *J. Phys. Chem. C,* 2013, 117, 19255–19269.

(40) Jin An, S.; Li, J.; Daniel, C.; Mohanty, D.; Nagpure, S.; Wood, D. L. The State of Understanding of the Lithium-ion-battery Graphite Solid Electrolyte Interphase (SEI) and its Relationship to Formation Cycling, *Carbon* 2016, 105, 52–76.

(41) Wu S.; Zhu K.; Tang J.; Liao K.; Bai S.; Yi J.; Yamauchi Y.; Ishida M.; Zhou H. A long-life lithium ion oxygen battery based on commercial silicon particles as anodes, *Energy Environ.Sci.,* 2016, 9, 3262-3271

TOC

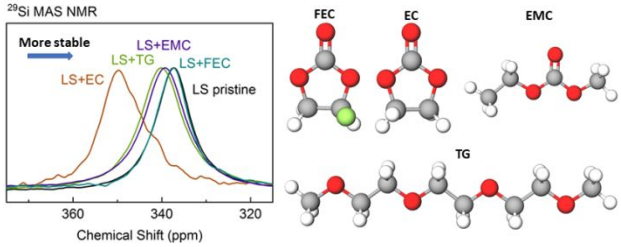
^{29}Si MAS NMR
More stable
LS+EMC
LS+TG
LS+FEC
LS+EC
LS pristine
360
340
320
Chemical Shift (ppm)
FEC
EC
EMC
TG